

# Theory for Roll-Ratchet Phenomenon in High-Performance Aircraft

Ronald A. Hess\*

University of California, Davis, Davis, California 95616

**Roll ratchet refers to a high-frequency oscillation that can occur in pilot-in-the-loop control of roll attitude in high-performance aircraft. The frequencies of oscillation typically are well beyond those associated with the more familiar pilot-induced oscillation. A structural model of the human pilot, which has been employed to provide a unified theory for aircraft handling qualities and pilot-induced oscillations, is employed here to provide a theory for the existence of roll ratchet. It is hypothesized and demonstrated using the structural model that the pilot's inappropriate use of vestibular acceleration feedback can cause this phenomenon, a possibility that has been discussed by other researchers. The possible influence of biodynamic feedback on roll ratchet also is discussed.**

## Introduction

FIGURE 1, taken from Ref. 1, shows two time histories involving the U.S. Air Force (USAF)/CALSPAN NT-33A variable-stability aircraft and the prototype YF-16 vehicle. As Fig. 1 indicates, high-frequency roll oscillations (12.17–12.5 rad/s) occurred under piloted control. Oscillations such as these have been termed roll ratchet by pilots and flight-control engineers. The term finds its origin in pilot descriptions of the event, i.e., pilots often describe what they perceive to be a ratcheting-like motion. The ratcheting sensation may be attributable to a threshold nonlinearity in the human middle ear, where acceleration is sensed. Although not a dangerous condition, per se, roll ratchet often precludes acceptable performance in air-to-air tracking tasks and almost invariably leads to a significant degradation in handling qualities ratings.

There has been a considerable amount of research devoted to seeking the mechanism behind the roll-ratchet phenomenon.<sup>1–6</sup> Perhaps one of the first explanations of the phenomenon was offered in Ref. 2 and discussed in some detail in Ref. 1. Smith et al.<sup>2</sup> were the first to suggest the importance of acceleration cues in catalyzing roll ratchet:

Suppose the pilot reverts to an abrupt input technique to demand the desired response more rapidly, creates high angular accelerations and then switches his closure to angular acceleration error, instead of bank angle error. Then with sufficient pilot gain, a ratcheting type oscillation of  $\approx 16$  rad/s results.

Although recognizing the importance of acceleration cues, other researchers<sup>3,5</sup> have maintained that the interaction of the pilot's neuromuscular system and the cockpit control inceptor are the important factors in understanding roll ratchet. Figure 2, taken from Ref. 3, shows the Bode plots of a series of measured pilot-vehicle transfer functions from a fixed-base simulation of a roll-tracking task when a force-sensing cockpit inceptor was being used, i.e., the force that the pilot applied was sensed and used as a command to the vehicle and/or flight-control system. The amplitude peaking evident just beyond 10 rad/s should be noted. To induce an oscillatory response, the phase lag at the frequency where this amplitude peak crosses the 0-dB line has to be reduced to  $-180^\circ$ . The authors hypothesize that the pilot's use of motion cues provides this phase-lag reduction. In Fig. 2, the  $0.1\omega \times 57.3$  is the phase lead provided by inner-loop roll-rate feedback. The authors conclude that avoiding the use of force-sensing cockpit inceptors can minimize the occurrence of roll ratchet, a conclusion also reached in Ref. 5.

More recent flight-test results have demonstrated that merely avoiding force command inceptors is not sufficient to prevent the

occurrence of roll ratchet. In Refs. 4 and 6, flight-test data from the USAF/CALSPAN NT-33A variable-stability aircraft demonstrated that roll ratchet can occur with position-sensing inceptors. The data from these references are particularly interesting in that pilot-vehicle transfer functions, such as that shown in Fig. 2, were measured in tracking tasks involving sum-of-sinusoids, roll-command inputs. The interpretation of these data, however, varies. That is, referring to the work of Refs. 3 and 5, there is some evidence that neuromuscular mode peaking is occurring with roll ratchet, but it is not always present in the transfer functions in which ratchet is occurring. This, of course, can be explained by the fact that ratcheting is a sporadic event and the describing functions are time-averaged linearizations of the entire tracking sequence. Thus, those periods when ratchet did not occur were averaged with those in which it did, and the result shows evidence of peaking, but no ratchet.

## Model-Based Theory for Roll Ratchet

### Introduction

The explanations for roll ratchet briefly described in the preceding paragraph, although plausible, require some rather special conditions to be met for their validity. For example, the theory forwarded in Refs. 1 and 2 requires the pilot to visually sense the second derivative of the system error, not an easy task based on what is known of human pilot visual-sensing capabilities. As mentioned in the preceding section, the theory of Ref. 3 requires the amplitude of the neuromuscular mode peak in the pilot-vehicle transfer function to be near or at unity (0 dB) at the frequency where the phase lag is near or at  $-180^\circ$ , with the latter condition created by the pilot's use of motion feedback.

The explanation to be proposed herein draws upon both of the previous approaches to some extent. However, it is based on a simple model of the human pilot, which has been used to provide a unified theory for aircraft handling qualities and pilot-induced oscillations (PIO).<sup>7</sup> As will be seen, with this model, the roll-ratchet phenomenon can be explained by the pilot's use of an inappropriately large feedback gain on roll acceleration sensed through the vestibular system.

### Revised Structural Model

Figure 3 shows what is referred to here as the revised structural model of the human pilot. The model has its genesis in a previously described structural model<sup>8</sup> and in a later modification of that model.<sup>5</sup> As shown in Fig. 3, the model is describing compensatory pilot behavior, i.e., behavior involving closed-loop tracking in which the visual input is system error. The elements within the dashed box represent the dynamics of the human pilot.

The model of Fig. 3 is discussed thoroughly in Ref. 7, and part of that discussion is repeated here for the sake of completeness. Starting from the left, one sees the system error  $e(t)$  following one of two possible paths. One path is intended to model the human's visual rate-sensing dynamics, here modeled by a differentiator  $s$ ,

Received March 14, 1997; revision received June 27, 1997; accepted for publication July 10, 1997. Copyright © 1997 by the American Institute of Aeronautics and Astronautics, Inc. All rights reserved.

\*Professor, Department of Mechanical and Aeronautical Engineering. Associate Fellow AIAA.

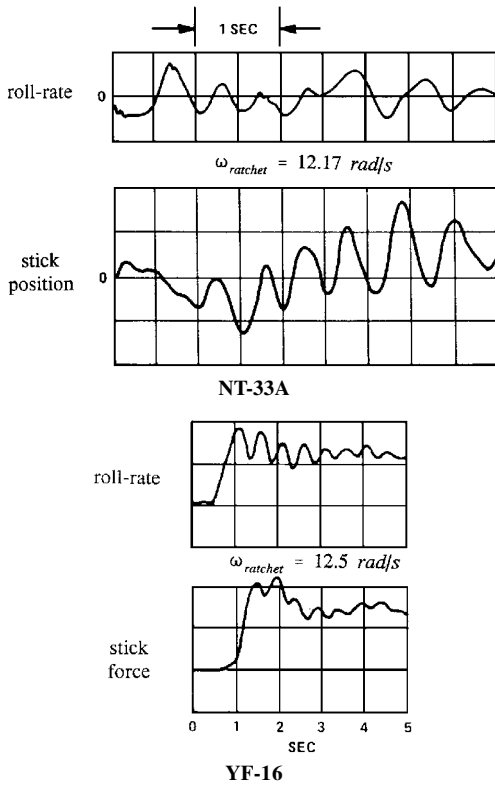


Fig. 1 Roll-ratchet time histories.

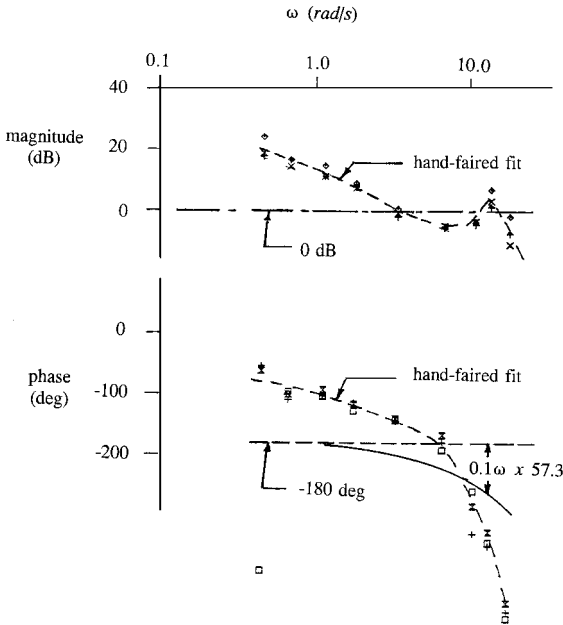


Fig. 2 Measured pilot-vehicle transfer-function characteristics from Ref. 3.

an injected noise signal, and a gain  $K_e$ . The remaining path describes normal error sensing and gain compensation  $K_e$ , including the possibility of the human's accomplishing low-frequency trim (or integral) compensation via  $\epsilon/s$ . In this study,  $\epsilon \equiv 0$ . The switch labeled  $S_1$  allows switching between error and error-rate tracking. This switching has been hypothesized to play a critical role in the initiation and sustenance of PIO.<sup>7</sup> Switches  $S_1$  and  $S_2$  are assumed to operate in unison, i.e., when  $S_1$  is in the "up" position, so is  $S_2$ . For this study, however, it is assumed that switches  $S_1$  and  $S_2$  remain in the "down" position and normal error sensing and compensation are used. A central-processing time delay  $\tau_0$  also is included. An inner, proprioceptive feedback loop is encountered next. In the forward portion of this loop, the elements  $Y_{NM}$  and  $Y_{FS}$  are intended to represent, respectively, the open-loop dynamics of the neuromuscular

system driving the cockpit inceptor and the dynamics of the inceptor force-feel system itself. The feedback portion of this loop contains the element  $Y_{PF}$ , which receives as its input the proprioceptively sensed inceptor output  $\delta_m(t)$ . The element  $Y_{PF}$  and its position in the model are central to the philosophy of the structural model, i.e., that the primary equalization capabilities of the human pilot are assumed to occur through operation upon a proprioceptively sensed, as opposed to a visually sensed, variable. The switch  $S_3$  allows either position-sensing or force-sensing inceptors to be modeled.

Time derivatives of the vehicle output  $m(t)$  are assumed to be individually sensed, as indicated in Fig. 3. Switch  $S_4$  allows either rate or acceleration cues, or neither, to be used in vehicular control. Note that feedback output rate is predicated on that signal creating an acceleration that can be sensed by the middle ear. In this study,  $K_{\ddot{m}} = 0$ . A visual feedback of vehicle output completes the model.

#### Model Parameterization

The reader is referred to Ref. 7 for a discussion of model parameterization, which is only summarized here. Elements  $Y_{NM}$  and  $Y_{PF}$  are given by

$$Y_{NM} = \frac{\omega_{NM}^2}{s^2 + 2\zeta_{NM}\omega_{NM}s + \omega_{NM}^2} \quad (1)$$

$$Y_{PF} = K(s+a) \quad \text{or} \quad K \quad \text{or} \quad K/(s+a) \quad (2)$$

with the particular equalization of Eq. (2) dependent on the form of the vehicle dynamics around the crossover frequency. The crossover frequency is chosen as 2.0 rad/s.

Nominal values for fixed model parameters can be given as

$$\tau_0 = 0.2 \text{ s} \quad \omega_{NM} = 10 \text{ rad/s} \quad \zeta_{NM} = 0.7 \quad (3)$$

The relatively simple relations of Eqs. (1-3), the crossover relation  $\omega_c = 2.0$  rad/s, and the selection of one of the three forms on the right-hand side of Eq. (2) allow implementation of the model of Fig. 3. The appropriate form in Eq. (2) is chosen so that the resulting open-loop transfer function,

$$Y_p Y_c(j\omega) = (\delta_M/E)(j\omega) \cdot Y_c(j\omega) \approx (\omega_c/j\omega)e^{-\tau_0 s} \quad \text{for } \omega \approx \omega_c \quad (4)$$

i.e.,  $Y_p Y_c(j\omega)$  follows the dictates of the crossover model of the human pilot.<sup>9</sup> The gain  $K$  appearing in Eq. (2) is chosen so that, with all other loops open, the minimum damping ratio of any quadratic closed-loop poles of  $(\delta_M/E_M)(s)$  is  $\zeta_{\min} = 0.15$ . Finally,  $K_e$  is selected so that the desired crossover frequency of 2.0 rad/s is obtained. As will be demonstrated, the inclusion of a nonzero  $K_{\ddot{m}}$  (with switch  $S_4$  in the up position) can alter the high-frequency characteristics of the open-loop transfer function  $(M/E)(s)$  and produce oscillatory behavior very similar to that seen in roll ratchet. The inclusion of a nonzero  $K_{\ddot{m}}$  after selection of  $K_e$  in the modeling procedure described in the preceding is possible because  $K_{\ddot{m}}$  has only a small effect on the crossover frequency.

#### Analysis of Roll Ratchet

##### Database

The data to be used are taken from those presented in Ref. 4 and discussed in Ref. 6. They involve a series of roll-tracking tasks conducted on the USAF/CALSPAN NT-33A variable-stability aircraft. Attention is focused on 11 configurations that have been identified in Ref. 6 as either not experiencing or experiencing roll ratchet during flight test. Figure 4 describes the shorthand notation used to identify the configurations. The 11 configurations analyzed are shown in Table 1.

It is useful to provide some validation of the structural model and parameter selection procedure described in the preceding section. To this end, a comparison can be made between a pilot-vehicle transfer function obtained from flight test and one generated by the structural model. Configuration 221P(18) was selected for comparison. Figure 5 shows the flight-test and model results. In terms of the variables in Fig. 3, Fig. 5 is a Bode plot of  $(M/E)(j\omega)$ . Shaded circles represent magnitude and phase measurements from flight test

at the frequencies of the command input sinusoids comprising  $c(t)$ ; solid and dashed curves represent the model results. The model was obtained using the pilot-vehicle analysis technique outlined in the preceding section with one exception: The crossover frequency for the model pilot-vehicle system was reduced from 2.0 rad/s to 1.5 rad/s to provide an acceptable match to the amplitude data and allow an easier comparison with these data. As Fig. 5 indicates, with the one exception of the crossover frequency, the comparison is quite

good. The crossover-frequency discrepancy was not deemed serious and is ignored in what follows.

Acceleration Feedback

The simple hypothesis offered here is that the roll-ratchet phenomenon can be induced by the pilot adopting an inappropriately large gain  $K_m$ . It is further hypothesized that this large gain is induced by rolling accelerations created by the aircraft and flight-control system that the pilot deems excessive for the task at hand. The latter hypothesis is identical to that offered in Refs. 1 and 2. The difference, however, is that the acceleration sensing occurs in a feedback loop through the vestibular system and is not occurring through visual means in the forward loop. The interplay of the neuromuscular system and the nature of the force-feel system are obvious from the structure of the proprioceptive feedback loop in Fig. 3. Thus, this hypothesis has many elements in common with that offered in Ref. 3. However, as demonstrated, only a single gain variation need be employed to induce a closed-loop oscillation very similar to a roll ratchet.

Table 1 Flight-test configurations analyzed from Ref. 4	
No roll ratchet	Roll ratchet
141F(10)	143P(18)
301P(18)	201P(18) + 55
302P(18)	221P(18)
341F(18)	301P(18) + 110
342P(18)	302P(18) + 55
342F(18)	

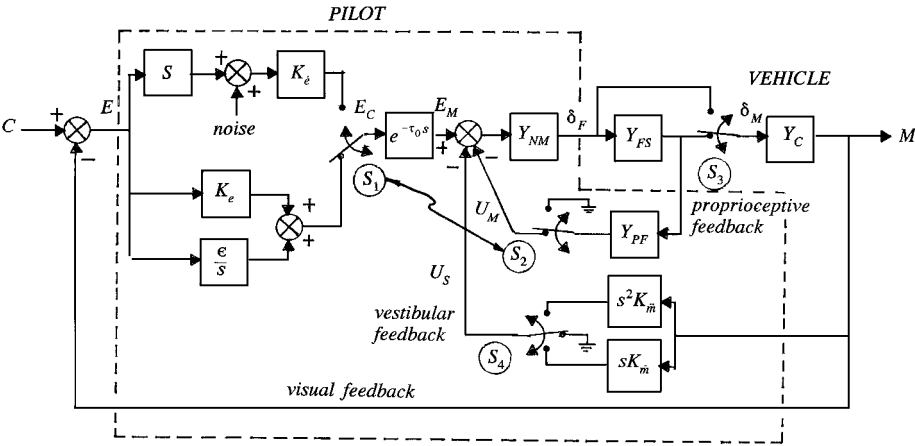
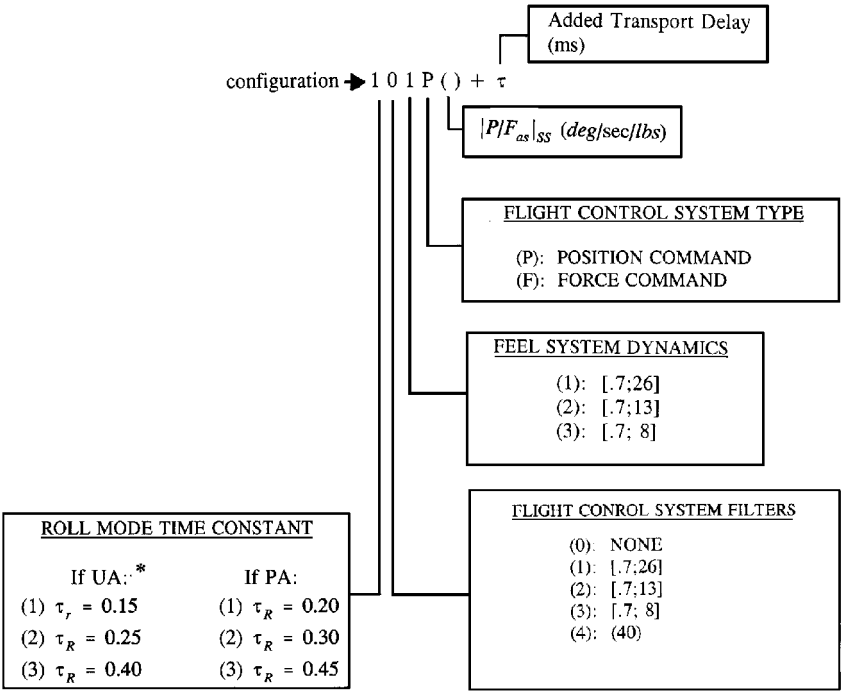


Fig. 3 Revised structural model of a human pilot.



\* UA = up and away flight  
PA = power approach

(a) =  $s+a$   
short-hand notation:  
 $[\zeta_n; \omega_n] = s^2 + 2\zeta_n \omega_n s + \omega_n^2$

Fig. 4 Configuration identification scheme from Ref. 6.

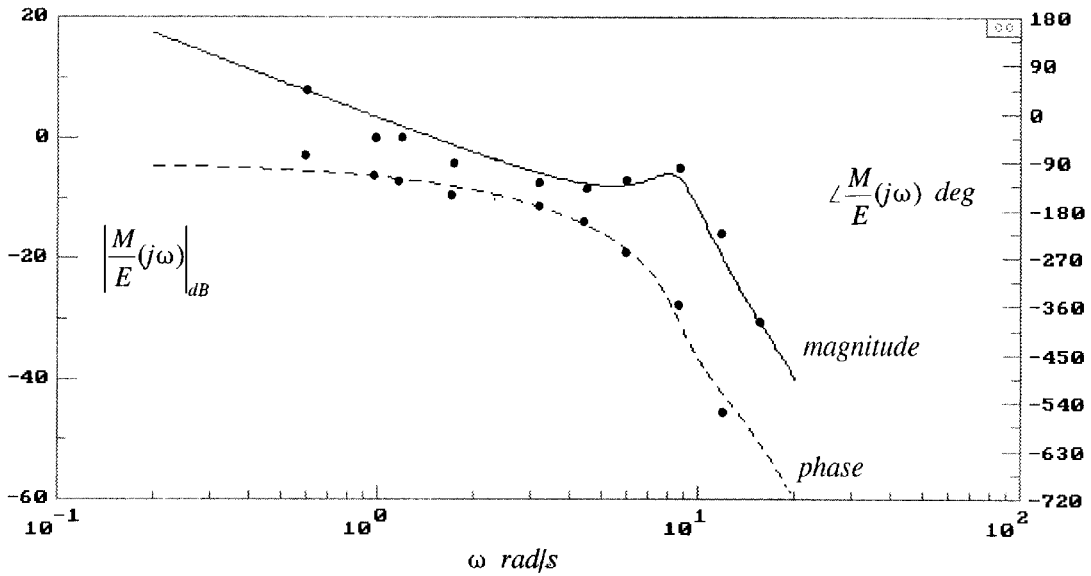


Fig. 5 Comparison of pilot-vehicle transfer functions from flight-test and structural model: configuration 221P(18).

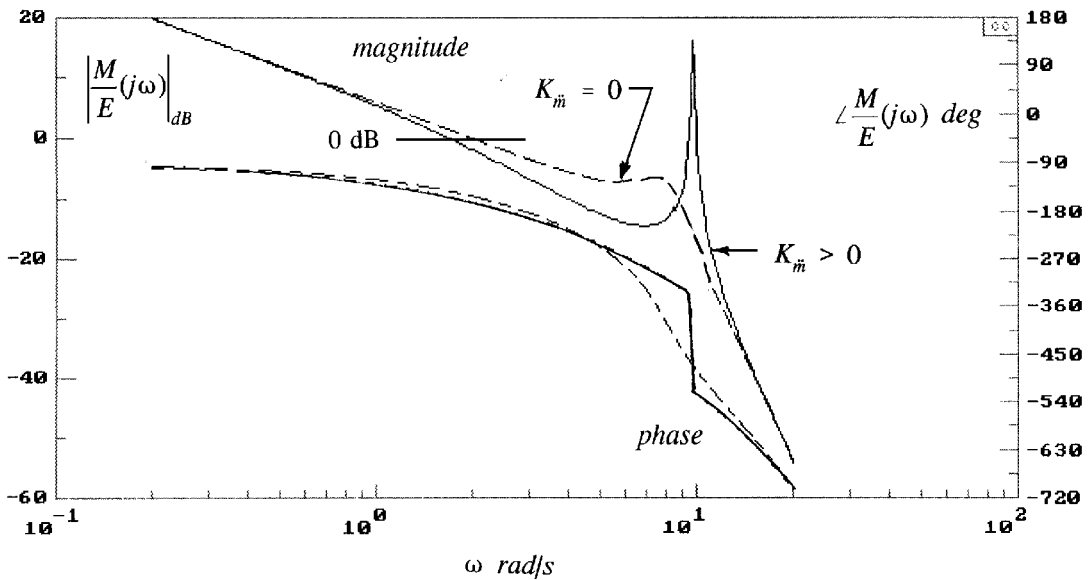


Fig. 6 Structural-model pilot-vehicle transfer function with two values of  $K_m$ : configuration 143P(18).

Figure 6 shows the structural-model pilot-vehicle transfer function for configuration 143P(18) with two values of  $K_m$ , zero and a value yielding a very lightly damped high-frequency mode. Note that such a gain increase may only be transient, i.e., it may not occur over a long enough period of time to be accurately captured by a single transfer-function measurement such as that shown in Fig. 5. Note also in Fig. 6 that there is only a modest change in crossover frequency with the nonzero  $K_m$ . Finally, the closure of the outer, visual loop in Fig. 3 has little effect on the relative stability of the oscillatory mode. This is shown in the root locus diagram of Fig. 7. Here, the open-loop transfer function  $(M/E)(s)$  includes the acceleration loop closed with the nonzero  $K_m$ . The small squares indicate closed-loop root locations, i.e., poles of the transfer function  $(M/C)(s)$ , for four values of the visual gain  $K_e$ . These correspond to factors of 1, 2, 5, and 10 times the nominal value that yielded the 2.0-rad/s crossover frequency with  $K_m = 0$ . Note the very small change in the position of the oscillatory roll-ratchet roots. Taking the model at face value, this result means that the pilot cannot stop a roll ratchet by varying his/her outer-loop visual gain  $K_e$ . The ratchet can be stopped only by a reduction in  $K_m$ . It is interesting to compare this result with that implied by Fig. 2 and Ref. 3. There, the existence of a roll ratchet is predicated upon an appropriate outer-loop gain

that forces the magnitude of the open-loop transfer function to be unity (0 dB) at the frequency at which the phase angle is  $-180$  deg. A similar statement can be made about the model proposed in Ref. 1.

Figure 8 shows the output  $m(t)$  and the force input  $\delta_F(t)$  to a unit step input for configuration 143P(18). This pair of time histories is interesting in that they are qualitatively similar to recorded roll-ratchet time histories. That is, only a small-amplitude oscillation is evident in roll attitude, whereas a large-amplitude oscillation is evident in control input. Figure 9 shows the pilot control force input during flight-test roll-ratchet encounter with configuration 143P(18). The frequency of oscillation is 10.4 rad/s, whereas that obtained with the model is 9.8 rad/s.

The inappropriately large gain  $K_m$  may be attributed to the following. In maneuvering, the particular flight configurations that are prone to roll ratchet create a rolling acceleration that the pilot finds excessive for the task at hand. This may occur even if the task itself involves relatively modest accelerations in an absolute sense. If a physiological sensor is available to measure this acceleration (which it obviously is), the natural tendency on the part of the pilot may be to feed back this variable and attempt to reduce it through control activity. However, because of the structure of the pilot's feedback

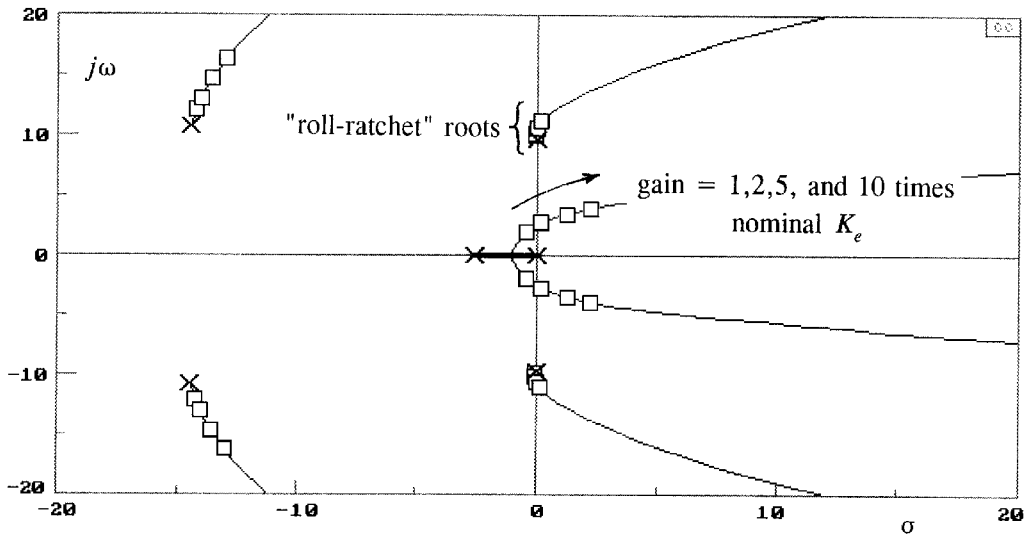


Fig. 7 Root locus diagram for closed-loop poles of  $(M/C)(s)$  with open-loop transfer function  $(M/E)(s)$  defined with nonzero  $K_m$  of Fig. 6. Closed-loop roots correspond to varying nominal  $K_e$  by factors of 1, 2, 5, and 10.

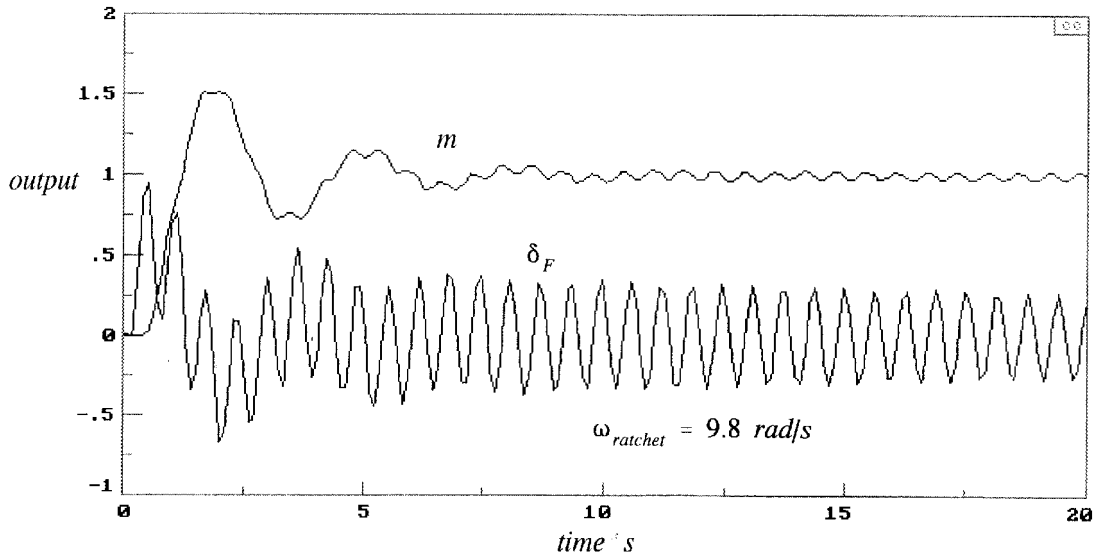


Fig. 8 Closed-loop step response of pilot-vehicle system of Fig. 3, with pilot-vehicle transfer function of Fig. 6.

system, this action merely leads to a very lightly damped mode and a roll ratchet.

#### Vehicle Characteristics

If initial acceleration response is involved in the initiation of roll ratchet, it may be possible to distinguish some differences in the open-loop acceleration response to applied force inputs, at least for the 11 configurations of Table 1. To this end, the transfer function

$$\left[ s^2 \cdot (M/\delta_F)(s) \right]_{s=j\omega}$$

was plotted for each set of configurations in Table 1, i.e., those with no ratchet and those with ratchet. No units are given in Figs. 10 and 11 because these plots are intended only for comparison among the configurations in Table 1. Note that this transfer function will contain just vehicle, actuator, and force-feel system dynamics when a position-sensing inceptor is being used and vehicle and actuator dynamics alone when a force-sensing actuator is being used; no pilot dynamics are included. Figures 10 and 11 summarize the results. Because it is the initial acceleration response that is of interest ( $t \ll 1$ ), attention should be focused on the characteristics of  $[s^2 \cdot (M/\delta_F)(s)]_{s=j\omega}$  for values of  $\omega$  that are large but do not exceed the upper limit of the frequency range of interest for manual control, i.e.,  $\omega \approx 10$  rad/s. Figure 10 shows  $[s^2 \cdot (M/\delta_F)(s)]_{s=j\omega}$  for the configurations that did not exhibit roll ratchet, whereas Fig. 11

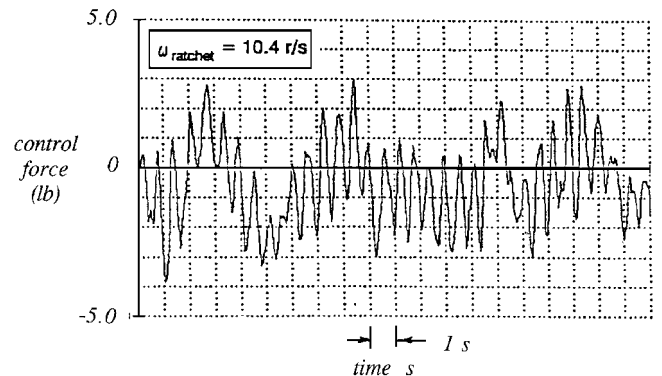


Fig. 9 Pilot inceptor force inputs from flight test of Ref. 4, as reported in Ref. 6, for configuration 143P(18).

shows the function for those that did. Even for this small data set, some basic differences appear. The no-ratchet cases all had phase lags at 10 rad/s that were less than  $-75$  deg, i.e., less negative. In contrast, all but one of the ratchet cases had phase lags greater than  $-75$  deg, i.e., more negative. The configuration in Fig. 11 that did not have a phase lag at 10 rad/s exceeding  $-75$  deg did, however, have a relatively large magnitude at this frequency. The magnitude and phase for this configuration [201P(18) + 55] are denoted by

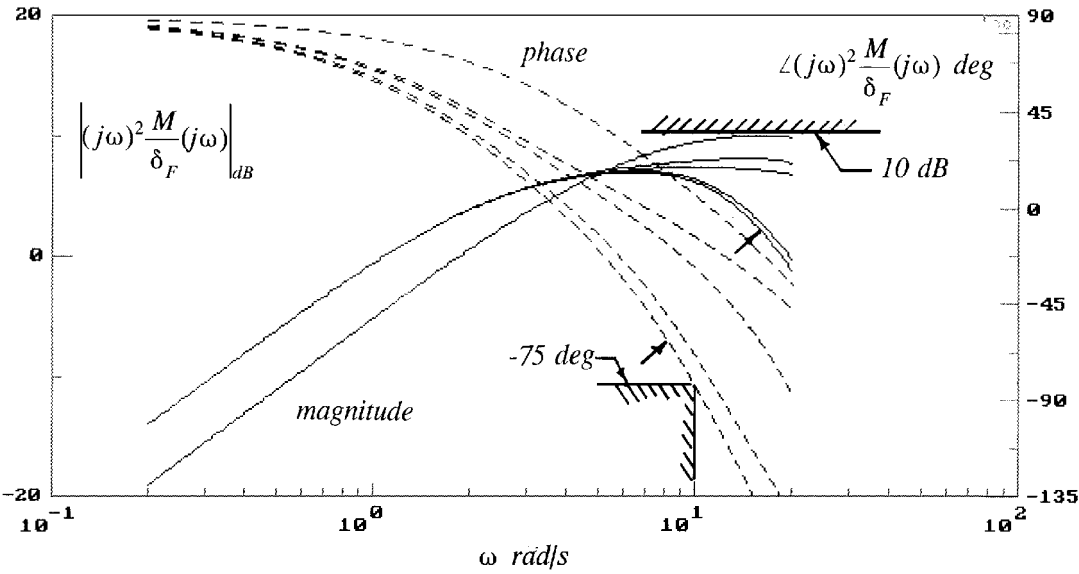


Fig. 10 Transfer function  $[s^2 \cdot (M/\delta_F)(s)]_{s=j\omega}$  for configurations in Ref. 6 identified as not experiencing roll ratchet.

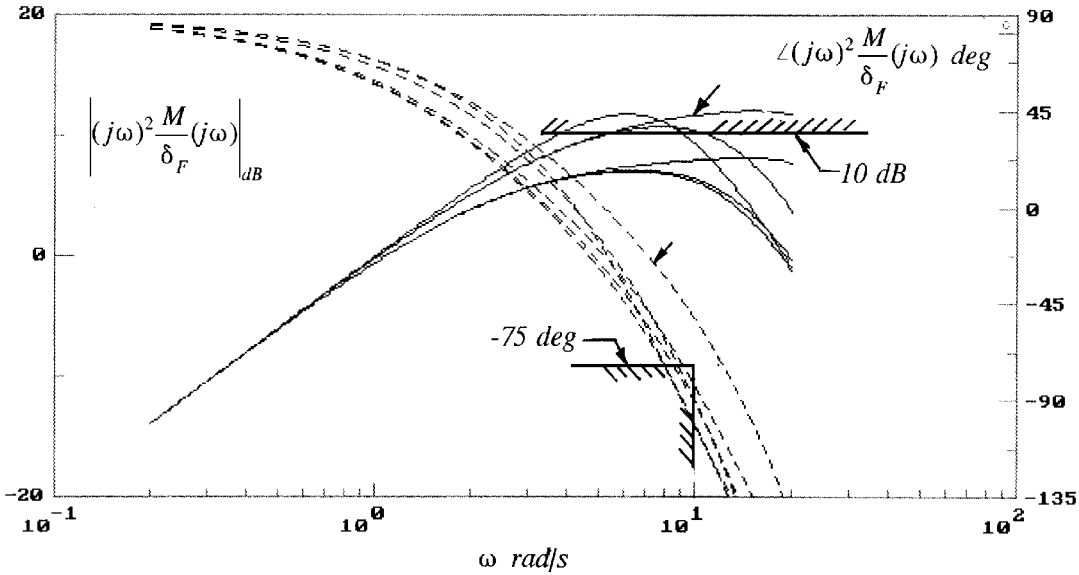


Fig. 11 Transfer function  $[s^2 \cdot (M/\delta_F)(s)]_{s=j\omega}$  for configurations in Ref. 6 identified as experiencing roll ratchet.

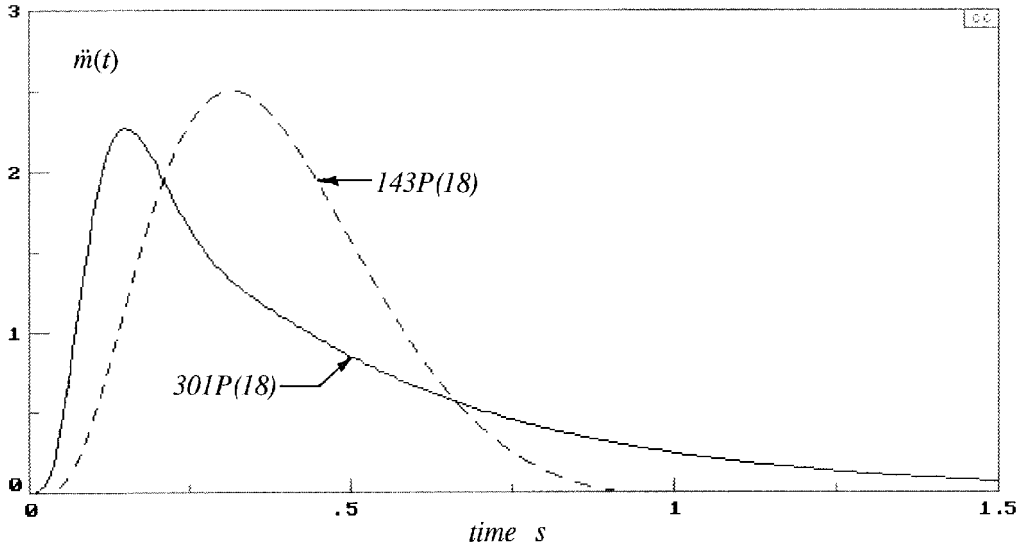


Fig. 12 Roll acceleration responses to step-force inputs for configurations 301P(18) (no ratchet) and 143P(18) (ratchet).

arrows in Fig. 11. The one configuration in Fig. 10 that comes close to exceeding  $-75$  deg [342P(18)] also exhibits the smallest magnitude in the high-frequency range. This pair also is denoted by arrows in Fig. 10. It is interesting that, of the two piloted evaluations of configuration [342P(18)] reported in Ref. 4, one of the pilots reported no roll ratchet and gave the configuration a Cooper-Harper rating of 2. The second pilot, however, did report some oscillation problems that he found objectionable but said that there were no (PIO) problems. He gave the configuration a Cooper-Harper rating of 5 because of these oscillations. It is not known for certain whether these oscillations were roll ratchet; however, one might expect that they were because the pilot explicitly exonerated the vehicle from PIO tendencies (which typically are categorized by pilots as being of lower frequency than roll ratchet). Thus, the close call for configuration 342P(18) in Fig. 10 may be reasonable. These results support a hypothesis that initial acceleration responses to force inputs that exhibit large lags or large amplitudes in the frequency domain may induce the pilot to employ an inappropriately large acceleration feedback gain in an attempt to control the resulting response. As an example of such responses in the time domain, Fig. 12 compares the time-domain roll acceleration responses to step-applied forces for configurations 301P(18) (no ratchet) and 143P(18) (ratchet). Figures 10 and 11 also show a pair of phase-amplitude boundaries that can be used to delineate the roll-ratchet proneness of these configurations. That is, if the magnitude or phase of  $[s^2 \cdot (M/\delta_F)(s)]_{s=j\omega}$  violates either of these bounds, the configuration experiences roll ratchet in flight test. Of course, it is presumed that some minimum magnitude of  $[s^2 \cdot (M/\delta_F)(s)]_{s=j\omega}$  at 10 rad/s would be required to induce roll ratchet. The relatively small data set of Table 1 does not permit an estimate of this lower bound.

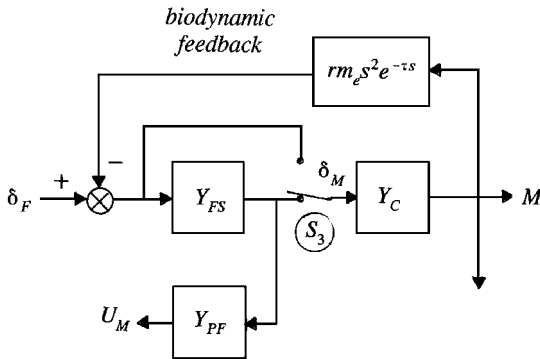


Fig. 13 Modification of Fig. 3 to model biodynamic feedback.

## Biodynamic Feedback

A discussion of roll ratchet would not be complete without considering the possible role that biodynamic feedback may play in the phenomenon. The term biodynamic or biomechanical feedback is used here to imply the effects that vehicle roll acceleration might have on the pilot's arm and cockpit inceptor and how these effects may serve to catalyze roll ratchet.

A very simple model of biodynamic feedback can be obtained by considering the pilot's hand/arm and the inceptor grip as consisting of an effective point mass  $m_e$  a distance  $r$  above the instantaneous roll axis of the aircraft.<sup>5</sup> Consider the situation in which both the control-stick pivot point and the location of the effective point mass are above the instantaneous roll axis of the aircraft. When the aircraft is undergoing a rolling maneuver with roll acceleration  $\ddot{\phi}$ , the force that the pilot must apply to keep the inceptor from moving relative to the cockpit is simply  $-rm_e\ddot{\phi}$ . One can consider the biodynamic element to be  $rm_e s^2 e^{-\tau s}$ , where the time delay  $\tau$  accounts, in a rudimentary way, for the phase effects of neglected higher-frequency dynamics in the biodynamic model. Figure 13 shows how the structural model of Fig. 3 can be modified to incorporate this rudimentary model of biodynamic feedback.

Figure 14 shows the root locus diagrams for the closed-loop poles of the  $(M/E_M)(s)$  transfer function from Fig. 3 or 13, with  $\tau = 0.025, 0.05$ , and  $0.1$  s with vehicle dynamics and model parameters ( $Y_{PF}$ ) for configuration 143P(18). The closed-loop poles in Fig. 14 correspond to those values of  $rm_e$  chosen to produce oscillatory roots with the gain  $K_{bd}$  normalized with respect to the oscillatory value for  $\tau = 0.025$  s. For the case in which  $\tau = 0.1$  s, the frequency of the oscillatory mode is 11.4 rad/s, close to the roll-ratchet frequency of 10.4 rad/s obtained in flight test for configuration 143P(18). An open-loop transfer function very similar to that indicated by the solid curves in Fig. 6 was obtained for the case with biodynamic feedback and  $\tau = 0.1$  s, a result that is not too surprising because the same variable is being fed back in both cases, albeit into different locations in the pilot model.

Figure 14 suggests that biodynamic feedback may itself produce oscillatory behavior of the kind and frequency associated with roll ratchet. However, one must bear in mind that the gain on the root locus diagrams of Fig. 14 is not a variable quantity as in the case of  $K_{\ddot{m}}$  but rather a geometrical/biomechanical constant, whose value is a function of the mass distribution of the control inceptor; the mass, position, and tension of the muscle groups subject to motion under acceleration; and the position of the aircraft's instantaneous roll axis. Although it is certainly possible that these quantities may produce oscillatory root locations, it would appear to the author to be less likely than in the case of acceleration feedback via  $K_{\ddot{m}}$ . Finally, note that conditions that would increase the likelihood of biodynamically

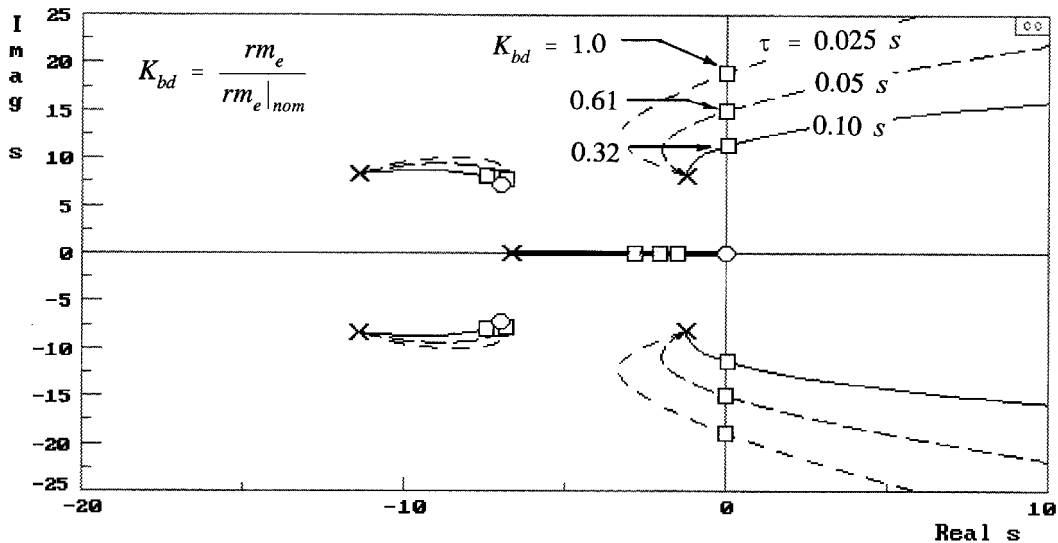


Fig. 14 Root locus diagrams for closed-loop poles of  $(M/E_M)(s)$  for different  $\tau$  values in biodynamic feedback model.

induced roll ratchet, e.g., lack of sufficient arm support and/or lack of a mechanical breakout in a control inceptor, are also conditions that would adversely affect the operation of the hypothesized proprioceptive loop in Fig. 3. This, in turn, could induce the pilot to use acceleration feedback in an attempt to ameliorate roll accelerations produced by control-stick inputs of less precision than desired.

### Discussion

The preceding analysis obviously is not exhaustive in terms of configurations analyzed. It is intended to demonstrate that a theory could be proposed to explain the origins of the roll-ratchet phenomenon that is consistent with previous observations and could be part of a larger theory that has attempted to unify aircraft handling qualities and the lower-frequency phenomena typically identified as PIO.<sup>7</sup> It is not proposed that the boundaries shown in Figs. 10 and 11 be considered as a metric for assessing the roll-ratchet proneness of any vehicle. In addition to the fact that these particular results have been scaled (no units given), the different vehicles will induce different accelerations to identical control-force inputs merely because of different pilot station locations. The fact that the 11 configurations of Table 1 were created on the same test vehicle made the comparisons of Figs. 10 and 11 possible. As stated in the preceding section, Figs. 10 and 11 merely support the idea that the characteristics of initial acceleration response may be a key factor in initiating roll ratchet. Finally, the possibility that biodynamic feedback may act as a catalyst for roll ratchet is certainly plausible but is felt to be a less likely explanation than the proposed theory.

### Conclusions

A theory for the roll-ratchet phenomenon can be forwarded that is based on a revised structural-pilot model. The theory states that roll ratchet is caused by the pilot's inappropriate use of vestibular acceleration feedback. The proposed theory contains elements found in previous explanations of roll ratchet, i.e., the importance of acceleration cues and the influence of the pilot's neuromuscular dynamics. Using the structural model, one can create oscillations whose frequency closely approximates that found in flight test of roll-ratchet-prone aircraft. In addition, the nature of the time histories that can be produced by the model are qualitatively similar to those found in flight test, i.e., small-amplitude oscillations in roll-attitude time histories, but strong evidence in control-input

time histories. As opposed to other model-based explanations for roll ratchet, the structural model implies that the pilot cannot halt a roll-ratchet encounter by changes in his/her visual gain but only by reduction in the vestibular-acceleration feedback gain. For the series of flight tests analyzed, the nature of the initial (open-loop) acceleration response of the vehicle could be used to categorize the roll-ratchet proneness in the 11 configurations chosen for study. Biodynamic feedback was modeled in rudimentary fashion and found to be a plausible but, in the author's opinion, less likely candidate for catalyzing roll ratchet. At present, the database is not sufficient to delineate between these alternative explanations or to corroborate a theory that draws upon both.

### Acknowledgments

This research was supported by NASA Langley Research Center under Grant NAG1-1744. Barton Bacon was the Contract Technical Manager.

### References

- <sup>1</sup>Chalk, C. R., "Excessive Roll Damping Can Cause Roll Ratchet," *Journal of Guidance, Control, and Dynamics*, Vol. 6, No. 3, 1983, pp. 218, 219.
- <sup>2</sup>Smith, R. E., Monagan, S. J., and Bailey, R. E., "An In-flight Investigation of Higher Order Control System Effects on the Lateral-Directional Flying Qualities of Fighter Airplanes," AIAA Paper 81-1891, Aug. 1981.
- <sup>3</sup>Johnston, D. E., and Aponso, B. L., "Design Considerations of Manipulator and Feel System Characteristics in Roll Tracking," NASA CR-4111, Feb. 1988.
- <sup>4</sup>Bailey, R. E., and Knots, L. H., "Interaction of Feel System and Flight Control System Dynamics on Lateral Flying Qualities," NASA CR-179445, Dec. 1990.
- <sup>5</sup>Hess, R. A., "Analyzing Manipulator and Feel System Effects in Aircraft Flight Control," *IEEE Transactions on Systems, Man, and Cybernetics*, Vol. 20, No. 4, 1990, pp. 923-931.
- <sup>6</sup>Mitchell, D. G., Aponso, B. L., and Klyde, D. H., "Effects of Cockpit Lateral Stick Characteristics on Handling Qualities and Pilot Dynamics," NASA CR-4443, June 1992.
- <sup>7</sup>Hess, R. A., "Unified Theory for Aircraft Handling Qualities and Adverse Aircraft-Pilot Coupling," *Journal of Guidance, Control, and Dynamics*, Vol. 20, No. 6, 1997, pp. 1141-1148.
- <sup>8</sup>Hess, R. A., "A Model for the Human's Use of Motion Cues in Vehicular Control," *Journal of Guidance, Control, and Dynamics*, Vol. 13, No. 3, 1990, pp. 476-482.
- <sup>9</sup>McRuer, D. T., and Krendel, E. S., "Mathematical Models of Human Pilot Behavior," AGARDograph-AG-188, Jan. 1974.